Carbon dioxide sequestration on mortars containing recycled aggregates: a hot area for startup development

7

M. Mastali [1], *Z. Abdollahnejad* [1], *F. Pacheco-Torgal* [1,2]
[1]C-TAC Research Centre, University of Minho, Guimarães, Portugal; [2]SHRC, University of Sungkyunkwan, Suwon, Republic of Korea

7.1 Introduction

According to Watts (2018), in February of last year, the temperatures in the Arctic remained 20°C above the average for longer than a week having increased the melting rate. As a consequence, the replacement of ice by water will lead to a higher absorption of solar radiation that makes oceans warmer being responsible for basal ice melting (Tabone et al., 2019) and also for a warmer atmosphere (Ivanov et al., 2016). This constitutes a positive feedback that aggravates the problem. Two years ago, Wadhams (2017) already stated that an ice-free Arctic will occur in the next few years, and that it will likely increase by 50% the warming caused by the CO_2 produced by human activity. The latest data on rates of melting combined with new models suggest that an ice-free Arctic summer could occur by 2030 (Screen and Deser, 2019; Bendell, 2018).The warming of the Earth will also result in extensive permafrost thaw in the Northern Hemisphere. With thaw, large amounts of organic carbon are mobilized, some of which is converted and released into the atmosphere as greenhouse gases. This, in turn, facilitates a positive permafrost carbon feedback and thus further warming. Turetsky reported that permafrost thawing could release between 60 billion and 100 billion tonnes of carbon. This is in addition to the 200 billion tonnes of carbon expected to be released in other regions that will thaw gradually. The world is closer to exceeding the budget (cumulative amount of anthropogenic CO_2 emission compatible with a global temperature−change target) for the long-term target of the Paris Climate Agreement than previously thought. And according to Xu et al. (2018), three lines of evidence suggest that global warming will be faster than projected in the recent IPCC special report. First, greenhouse gas emissions are still rising. Second, governments are cleaning up air pollution faster than the IPCC and most climate modelers have assumed. But aerosols, including sulfates, nitrates, and organic compounds, reflect sunlight so the aforementioned cleaning could have a warming effect by as much as 0.7°C. And in third place, there are signs that the planet might be entering a natural warm phase because the Pacific Ocean seems to be warming up, in accord

Start-Up Creation. https://doi.org/10.1016/B978-0-12-819946-6.00007-2

with a slow climate cycle known as the Interdecadal Pacific Oscillation that could last for a couple of decades. And these three forces reinforce each other. Therefore, some authors (Hansen et al., 2017) state that carbon dioxide sequestration is crucial so targets for limiting global warming can be achieved. That is why carbon sequestration constitutes one of the Grande Challenges of Engineering (Mote et al., 2016). Europe is now putting great efforts and funding in carbon sequestration materials and technologies. The flagship program EnCO_2re, with public launch in 2016, currently looks to develop new technologies offering novel ways to use CO_2; increase awareness for CO_2 reuse; and ensure sustainability and social acceptance of materials and products by integrated socioecological research. Also carbon capture and sequestration is one of the 100 Radical Innovation Breakthroughs for the future (Europe, 2019). Currently, this carbon sequestration is carried out mostly through geologic CO_2 storage in saline aquifers (Zhang and Huisingh, 2017). However, that constitutes a passive strategy has large risks and also has a very high cost. Carbon capture and storage from the stream of concentrated CO_2 at fossil fuel burning sites like power plants or steel plants is more efficient and thus less expensive than direct air capture (Hansen et al., 2017). As a consequence, it is important to study how CO_2 generated by power plants and other facilities can be sequestrated in valuable products.

Several authors (Bertos et al., 2004; Jang et al., 2016) have studied the use of CO_2 as accelerated curing of cementitious construction materials. This technology will in future prevent carbon dioxide to be released into the atmosphere but also to accelerate curing and strength development of those materials. However, so far no studies were performed using alkali-activated−based materials. These materials are produced through the reaction of an aluminosilicate powder with an alkaline activator, usually composed by hydroxide, silicate, carbonate, or sulfate leading to the formation an amorphous aluminosilicate gel and secondary nanocrystalline zeolite-like structures (Provis, 2014). These materials have a particular ability for the reuse of several types of wastes (Payá et al., 2014; Bernal et al., 2016). Some wastes like fly ash deserve a special attention because they are generated in a very high amount and have a very low reuse rate. United States has a reuse rate for fly ash of around 50% meaning that 30 million tons of fly ash are not reused annually (ACAA, 2016). Waste glass is also a waste that is generated in relevant quantities and that merits increase recycling efforts. In 2010, approximately 425,000 tons of waste glass was produced in Portugal and only 192,000 tons were recycled. In Hong Kong, approximately 373 tons of waste glass is generated daily in 2010. The high volume of construction and demolition wastes (CDWs) also constitutes a serious problem. Eurostat estimates the total for Europe of around 1000 million tons/year, representing an average value of almost 2.0 ton/per capita. The reuse of CDW as recycled aggregates not only constitutes a way to give value to a waste but also prevents the use of river sand being necessary to achieve the 70% target until 2020 in EU (Pacheco-Torgal et al., 2013). Furthermore, the use of cementitious building materials reinforced with natural fibers could be a way to achieve a more sustainable construction. Natural fibers are a renewable resource and are available almost all over the world. Vegetable fibers and cement-based composites are as stronger as composites based on synthetic fibers, cost-effectiveness, and above all are environmental friendly (Pacheco-Torgal and Jalali, 2011). Moreover, their

environmental impact is lower than traditional building materials because relatively large amounts of atmospheric CO_2 can be sequestrated through photosynthesis (Shea et al., 2012). Among the new vegetable fibers used, hemp stands out from the rest because of its wide availability, low requirements of fertilizer and irrigation, good humidity control and favorable energy, and ecological balances (Zermenno et al., 2016). That is why research on cement composites reinforced by natural fibers constitutes an important trend in the sustainability context (Onuaguluchi and Banthia, 2016). Natural fibers can degrade in high alkaline environment of Portland cement composites (Gram, 1983). However, several authors (Agopyan et al., 2005; Tonoli et al., 2010) showed that carbonation is associated with a lower alkalinity that can help preserve both the properties and durability of composites reinforced with natural fibers. This means that accelerated carbonation of composites reinforced with natural fibers has not only carbon sequestration advantages but is also especially indicated for such composites. This paper discloses results of an investigation concerning the performance of fly ash/waste glass alkaline–based mortars with recycled aggregates reinforced by hemp fibers exposed to accelerated carbon dioxide curing.

7.2 Experimental program

7.2.1 Materials

The mortars were made of fly ash (FA), calcium hydroxide (CH), waste glass (MG), ordinary Portland cement (OPC), recycled aggregates, and a sodium hydroxide solution. The fly ash was obtained from The PEGO Thermal Power Plant in Portugal and categorized as class B and group N regarding the ASTM C618-15. Table 7.1 presents the major oxides of fly ash particles. The Portland cement is of type I class 42.5R from SECIL, its composition contains 63.3% CaO, 21.4% SiO_2, 4.0% Fe_2O, 3.3% Al_2O_3, 2.4% MgO, and other minor components. The calcium hydroxide was supplied by LUSICAL H100 and contains more than 99% CaO. Waste glass from glass bottles ground for 1 hour in a ball mill was also used. The final density of the milled waste glass was 1.27 g/cm^3. Solid sodium hydroxide was supplied by ERCROS, S.A., Spain, and was used to prepare the 8M NaOH solution. Distilled water was used to dissolve the sodium hydroxide flakes to avoid the effect of unknown contaminants in the mixing water. The NaOH mix was made 24 h prior to use in order to have a homogenous solution at room temperature. A recycled sand to binder ratio of 4 was used in all the mixtures. The recycled sand was obtained from the crushing of concrete blocks. The

Table 7.1 Chemical composition of major oxides in fly ash.

Material	Oxides (wt.%)							
	SiO_2	Al_2O_3	Fe_2O_3	CaO	MgO	Na_2O	K_2O	TiO_2
Fly ash	60.81	22.68	7.64	1.01	2.24	1.45	2.70	1.46

average compressive strength of concrete blocks was around 40 MPa. A preliminary sieving operation was carried out to remove both coarser and dust particles before being used. The dimension of the sieves was 4.75 and 0.6 mm. The sand was dried at 105°C for 24 h until constant mass was achieved. After the preliminary sieving, a standard sieving was carried out showing that the recycle sand has a fineness modulus of 3.885. The detailed grain size distribution of the recycled sand is presented in Fig. 7.1. The recycled sand has a water absorption by immersion of 13% having being determined with a 24-h saturation according to EN 1097-6. Before use the recycled sand was carbonated in a carbon chamber from Aralab model Fitoclima S600 (4.2% CO_2, 40% RH, and 20°C) for 48 h. The recycled sand has a water absorption of 25%. The explanation for the increase of the water absorption relates to the fact that when CSH carbonates its Ca/Si ratio drops and it becomes highly porous. Studies by NMR spectroscopy indicate that decomposition of C−S−H caused by carbonation involves two steps: (1) a gradual decalcification of the C−S−H, where calcium is removed from the interlayer and defect sites in the silicate chains until Ca/Si = 0.67 is reached, ideally corresponding to infinite silicate chains; (2) calcium from the principal layers is consumed, resulting in the final decomposition of the C−S−H and the formation of an amorphous silica phase (Savija and Lukovic, 2016). The mortars were reinforced by different weight percentage of hemp shiv fibers that were supplied by Canapor. No surface treatment was used for the hemp shiv fibers in order to avoid cost increase and maintain its eco-effectiveness. Table 7.2 shows the composition of calcined hemp. The characterization of hemp shiv fibers was implemented based on a statistical analysis to evaluate the variability of the fiber length, which was defined by using 200 fibers. Regarding the statistical analysis, most fiber lengths varied in the range of 20−30 mm (Fig. 7.2).

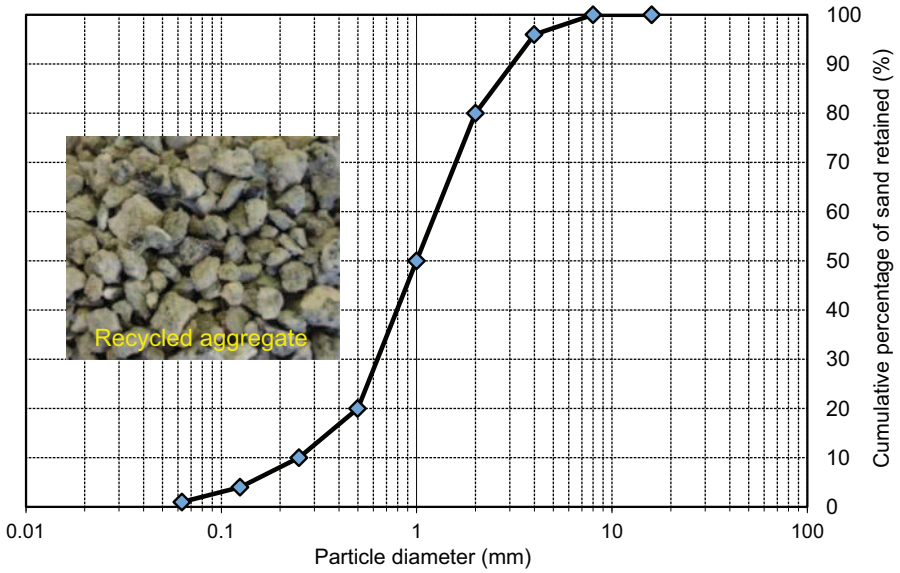

Figure 7.1 Distribution of sand particles.

Table 7.2 Chemical composition of major oxides in calcined hemp.

Material	Oxides (wt.%)							
	SiO_2	SO_3	P_2O_5	CaO	Fe_2O_3	Na_2O	K_2O	Mg
Calcined hemp	24.6	4.60	3.0	44.0	0.78	9.78	12.10	0.40

Figure 7.2 Hemp shiv fibers.

7.2.2 Mix design and mortar production

The composition of the mortars is shown in Table 7.3. In the batching process of the mortars, dry ingredients (fly ash, recycled sand, calcium hydroxide (or cement), metakaolin, and milled glass) were mixed for 2 min. Then, sodium hydroxide was added and again mixed for 3 min. Finally, the hemp fibers were added and all the ingredients were mixed for 3 more minutes. Then, the mixed mortars were cast into cubic molds ($50\ mm^3 \times 50\ mm^3 \times 50\ mm^3$) to assess the compressive strength and in prismatic beams with dimension (40 mm × 40 mm × 160 mm) to assess the flexural strength. The specimens were cured for 24 h at the lab conditions (averagely 25°C and 40% RH) and then they were demolded. Then the specimens were cured in the carbonation chamber (4.2% CO_2 concentration and 40% RH) for 7 days and curing in the lab conditions for the remaining days until the age of the test. This is because preliminary experiments showed that all mixtures were fully carbonated during 7 days through a CO_2 preconditioning curing. Three specimens with dimension of $50\ mm^3 \times 50\ mm^3 \times 50\ mm^3$ were casted and used to measure the CO_2 sequestration in the mixture without hemp fibers by using a furnace decomposition method (El-Hassan and Shao, 2015). The carbonated specimens were placed initially in the

Table 7.3 Proportions of mix compositions (kg/m^3).

Mixtures	Fly ash	CH	MG	SH	Sand	Molarity (mol/L)	Hemp fiber
80FA_10CH_10MG_RAGC_8M_0%	340.0	42.5	42.5	215.5	1700.0	8	0.0
80FA_10CH_10MG_RAGC_8M_4%							17.0
80FA_10CH_10MG_RAGC_8M_6%							25.5
80FA_10CH_10MG_RAGC_8M_8%							34.0

CH, calcium hydroxide; *FA*, fly ash; *MG*, milled glass; *SH*, sodium hydroxide.

oven at 105°C during 24 h to evaporate any absorbed water. Then, the weights of the dried specimens were recorded. Afterward, the specimens were put in the calciner at a temperature between 500 and 850°C during 4 h to measure the water bound to hydration products and carbon dioxide in carbonates. The results revealed that 800°C could be used as the appropriate decomposition temperature. The compressive strengths of the mixtures were assessed at different ages of 7, 14, and 28 days. The compressive strength of each mixture was obtained by averaging the replicated three cubes. All cubic specimens were assessed under compressive load with a constant displacement rate of 0.30 N/mm^2.s, based on the ASTM C109 recommendation. The compressive load was measured with a load cell of 200 kN capacity. Flexural performance was assessed under three-point bending (TPB) load conditions, as indicated in Figs. 7.3 and 7.4. The flexural load was applied to the beams with a displacement rate of 0.6 mm/min. The flexural load was measured with a load cell of 50 kN capacity. Eq. (7.2) was used to calculate the flexural strength of specimens under TPB test:

$$\sigma_f = \frac{3FL}{2bh^2} \tag{7.2}$$

where F is the total flexural load, L is span length, b and h are width (40 mm) and height (40 mm) of beams, respectively. Freeze/thaw resistance was assessed using three cubic specimens per mixture with dimension 100 mm × 100 mm × 100 mm were cast and tested after 28 days under compressive test. The equipment for freeze−thaw is Aralab model Fitoclima 1000. The freeze−thaw test was carried out according to PD CEN/TS 12390−9:2016 standard with temperatures ranged from −18 to +20°C. The specimens were kept 13 h in −18°C and 3 h in +20°C. The transitions from positive to negative and negative to positive temperatures took 3 and 5 h, respectively. Fig. 7.6 shows a freeze−thaw cycle. The specimens were submitted to 50 cycles.

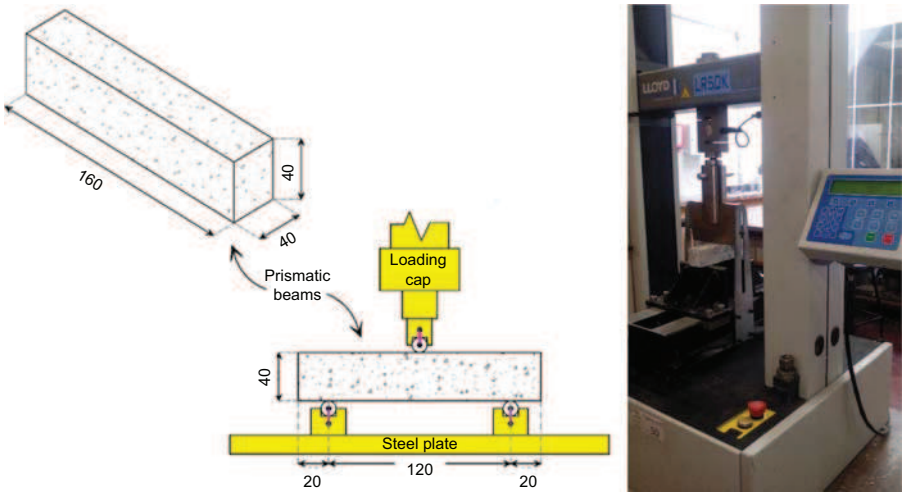

Figure 7.3 Adopted test setup for implementation of the flexural test.

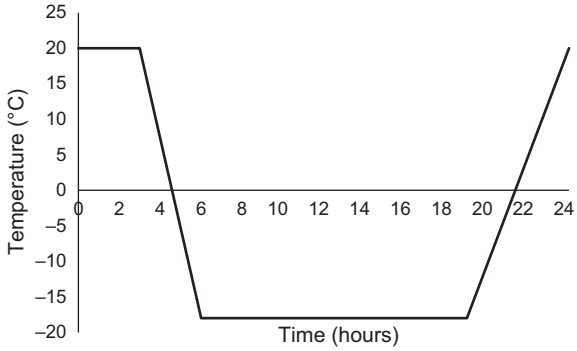

Figure 7.4 Temperature variation for one freeze/thaw cycle.

7.3 Results and discussion

7.3.1 Compressive strength

Fig. 7.5 shows the effects of different hemp shiv fiber contents on the compressive strength of fly ash—based alkaline mortars according to curing age. At 7 days, the reference mixture without fibers shows a compressive strength of about 7 MPa. This compressive strength level is lower for a structural application but is enough for masonry units. The use of accelerated carbonation makes CO_2 to diffuse through the pore network of the material, dissolving in the pore solution to form HCO_3-. This anion is a weak acid that will react with calcium-rich hydration products promoting the formation of calcium carbonates through a decalcification process (Bernal, 2014). The main calcium-rich hydration product is C—S—H because this study used a low sodium hydroxide concentration (Garcia-Lodeiro et al., 2016). The results show that the addition of hemp fibers leads to a reduction of compressive strength because fibers increase the porosity. This was also confirmed by other authors who studied the performance of composites containing hemp fibers (Li et al., 2006). For a hemp fiber content of 4%, a 20% reduction on compressive strength is noticed, while for an 8% fiber content, a 45% reduction on compressive strength is noticed. At 14 curing days, the reference mixture shows an increase of compressive strength of around 9 MPa representing a 30% increase concerning 7 days curing. From 14 curing to 28 curing days, a 10% increase in compressive strength was also noticed. At 28 curing days, the strength loss remains at 20% when 4% hemp fibers are used. However, the use of a hemp fiber content of 8% shows a low compressive strength when compared to 7 days curing it increased only 10% in compressive strength. It seems that a certain amount of hemp fibers can prevent the hydration products to become denser. Sedan et al. (2008) have reported that pectin can in fact fix calcium preventing the formation of CSH. Some studies show that hemp fibers have a pectin content of around 7.9% (Balciunas et al., 2015). Recent studies (Diquelou et al., 2015) also confirm that hemp fibers act as retarding agents, reducing compressive and flexural strength. The results of the present

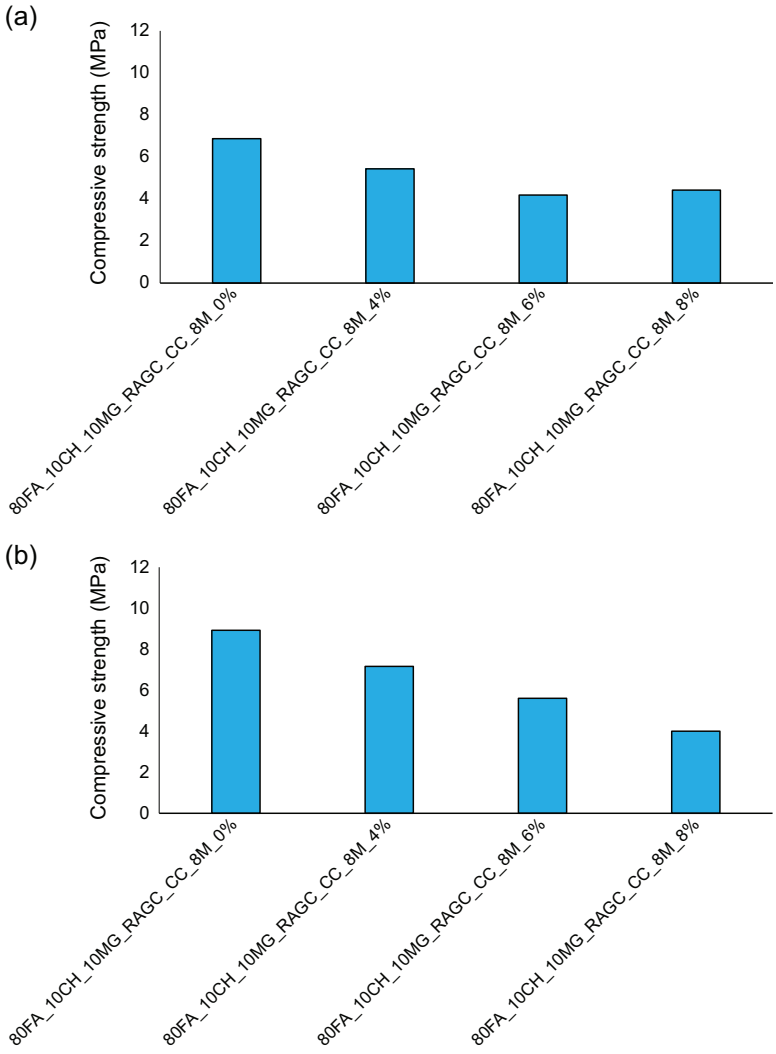

Figure 7.5 Compressive strength of mixtures cured for (a) 7 days; (b) 14 days; and (c) 28 days.

investigation show that 6% hemp fiber is the maximum content for masonry applications. Valle-Zermeño et al. also investigated the mechanical properties of magnesium phosphate cements reinforced with hemp fibre. The Hemp fibre percentages studied included 8%, 12%, 16%, and 20% total weight of dry ingredient. For a hemp fibre content of 8% they noticed a severe compressive strength reduction of from 30 MPa to just 10 MPa after 1 curing days and from 45 MPa to 12 MPa at 28 days. This severe reduction on compressive strength may be related to the fact that the high alkaline environment of the mixtures may degrade the structure of the fibers.

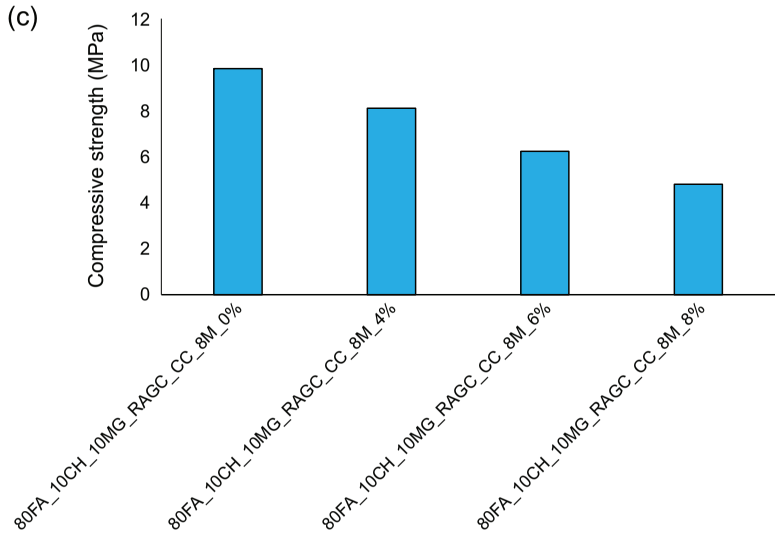

Figure 7.5 cont'd.

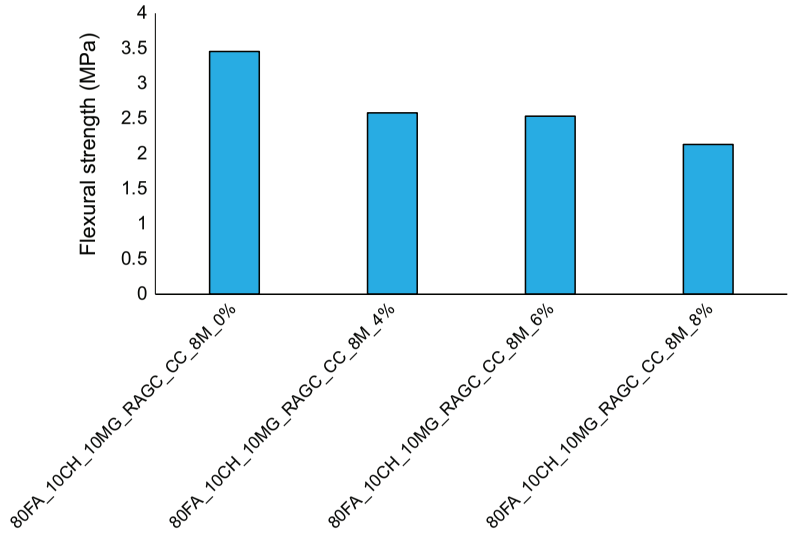

Figure 7.6 Flexural strength.

7.3.2 Flexural strength

Fig. 7.6 shows the effects of reinforcing fly ash alkaline-based mortars containing recycled aggregates with hemp shiv fibers at 28 curing days. Regarding the results, addition of fibers consistently reduced the flexural strength due to nonhomogeneous mix and, consequently, a poor adhesion between the fibers and the matrix. The use of just 4% of hemp fibers leads to flexural strength loss of about 25%. The maximum reduction in the flexural strength due to the addition of fiber was detected bout 40% in the mixture containing 8% hemp fiber (2.13 MPa), as compared to the plain mixture (3.45 MPa). Fig. 7.7 shows relevant correlations between the mechanical properties and the hemp fiber content. F_r denotes the flexural strength and W_f is the weight of hemp fiber. A high correlation ($R^2 = 0.86$) between compressive strength and flexural strength is noticed. A higher negative correlation ($R^2 = 0.97$) was found between compressive strength and hemp fiber content.

7.3.3 Resistance to freeze–thaw

Fig. 7.8 shows the results of compressive strength of reference mixtures cured at ambient temperature and the compressive strength of mixtures after 50 cycles of freeze/thaw. The results show that the mixtures with fiber content show a lower frost resistance when compared to the mixture without fibers. After 50 cycles of freeze/thaw, the mixture with no fiber shows a compressive strength loss of just 10%, while the mixtures with fibers show a compressive reduction of around 18%. The fiber content shows no direct influence regarding frost resistance. When water freezes in the pores of the matrix, an expansion in the volume of frozen water occurs, forcing the amount of excess water through the boundaries. The magnitude of this hydraulic pressure depends on the permeability of the matrix, the degree of saturation, the distance to the nearest unfilled void, and the rate of freezing, so that this hydraulic pressure exceeds the tensile strength of the paste, it forms the cracks. On further freezing cycles, new cracks will be formed and the deterioration will proceed.

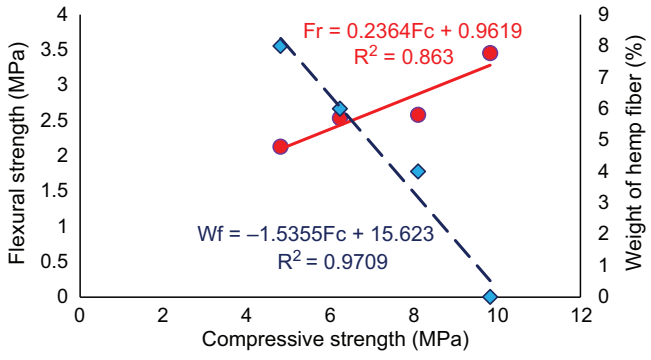

Figure 7.7 Correlation between compressive strength, flexural strength, and hemp fiber content.

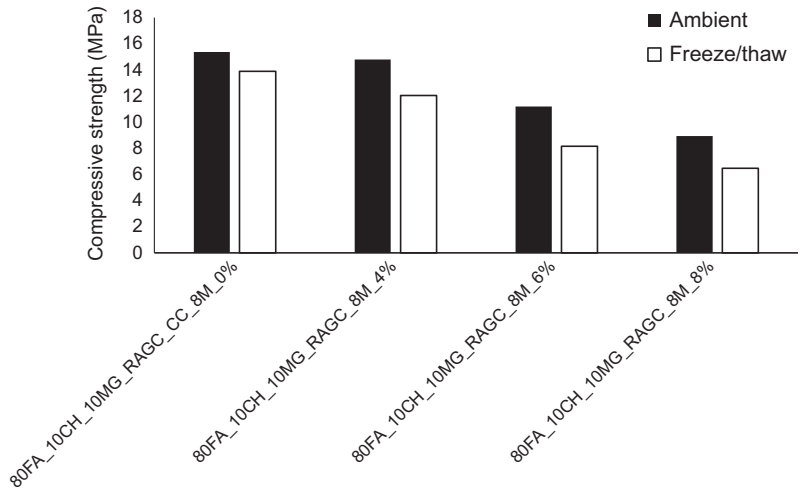

Figure 7.8 Effects of freeze/thaw on the compressive strength.

7.3.4 Carbon footprint

The global warming potential (GWP) of the different mixtures was calculated using the individual GWP values taken from the Ecoinvent database (Table 7.4). Details on the use of Ecoinvent database to estimate GWP on alkali-activated binders can be found in Ouellet-Plamondon and Habert (2014). The exception being the negative GWP of hemp fibers that was taken from the recent work of Arrigoni et al., (2017) and that is explained by the biogenic CO_2 uptake during hemp production. As to the carbon sequestration due to accelerated carbonation by using a furnace decomposition method it revealed a value of −102 $kgCO_2eq/m^3$. Fig. 7.9 shows the carbon footprint as well as the carbon sequestration. The results show that the carbon sequestration provided by the accelerated carbon curing has led to a carbon footprint of just 38 $kgCO_2eq/m^3$ for the mixtures without hemp fibers. Ouellet-Plamondon and Habert (2014) reported an embodied carbon of 227 $kgCO_2e/m^3$ for a mixture of hybrid cement−based concrete. Also Abdollahnejad et al. (2017) reported global warming potential in range of 178 and 250 $kgCO_2e/m^3$ for one-part geopolymer foam mortars composed of fly ash, Ordinary Portland cement, calcined kaolin, sodium hydroxide, and $Ca(OH)_2$.

Table 7.4 Global warming potential of each component of mixture ($kgCO_2eq$).

Recycled aggregates	MG	CH	Fly ash	Water	PC	SH	Hemp fiber
0.00401	0.00526	0.416	0.00526	0.000155	0.931	2.24	−1.70 Arrigoni et al. (2017)

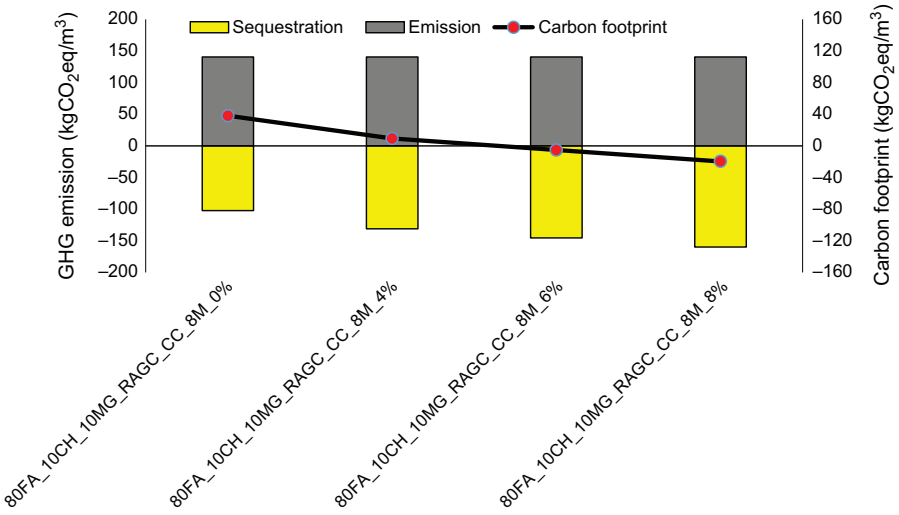

Figure 7.9 Greenhouse gas (GHG) emission and carbon footprint of different mixtures.

Those results confirm the very promising performance of the mixtures developed in this study. The use of hemp fibers leads to a sustained increase of carbon sequestration and a reduction of carbon footprint. Just using 6% hemp fibers leads to negative carbon dioxide footprint (-5.3 $kgCO_2eq/m^3$). Mixtures with 8% hemp fiber content show a carbon footprint of -19.7 $kgCO_2eq/m^3$.

7.3.5 Cost analysis

The construction industry has a very strong focus on cost and the fact that authors conducting studies on construction materials almost never address this issue has been one of the causes that makes the scientific community to develop materials that are never used due to cost restrictions. Furthermore, in a context of carbon sequestration, it is especially important to simulate how a future carbon tax will help favor products that have a high carbon sequestration potential. The cost of mixtures was calculated regarding the listed prices of mixture's ingredients in Table 7.5, which were provided by their suppliers. Moreover, two different scenarios were also assumed to consider a future carbon tax, including (1) 0.0347 Euro/kg for the carbon footprint as the first scenario (Stanford Report, 2015) and (2) 0.206 Euro/kg for considering the carbon

Table 7.5 Costs of the materials (Euro/kg).

Recycled aggregates	MG	CH	Fly ash	Water	PC	SH	Hemp fiber
0.047	0.009	0.283	0.03	0.01	0.1	0.85	0.52

footprint of mixtures as the second scenario (Moore and Diaz, 2015). Fig. 7.10 depicts the cost of the mixtures containing different masses of the hemp fibers. The mixture without hemp fibers has a cost of 160 euro/m^3. The hemp fiber addition led to a slight increase in the cost of about 5% to a 4% fiber content. The results also show that use of a carbon tax has almost no influence at all in the cost of the mixtures with negative carbon footprint.

7.4 Conclusions

Compressive strength and flexural strength were reduced by adding the hemp fiber, so that the maximum degradation in mechanical properties was found about 50% in the compressive strength due to addition of 8% hemp shiv fiber. The results show that 6% hemp fiber is the maximum content that allows a mechanical performance sufficient for masonry applications. A high correlation was found between compressive and flexural strength. A negative correlation was found between compressive strength and hemp fiber content. Accelerated carbonation showed a carbon sequestration of -102 $kgCO_2eq/m^3$ and a carbon footprint of 38 $kgCO_2eq/m^3$ for fly ash−based alkaline mortars. Increasing the hemp fiber consistently increased the CO_2 sequestration, so that the CO_2 sequestration varied in the range of -131 to -160 $kgCO_2eq/m^3$. Addition of the hemp fiber continuously reduced the carbon footprint, so that the carbon footprint in the mixture reinforced with 8% hemp fiber is around -19.7 $kgCO_2eq/m^3$. The results show that use of a carbon tax has almost no influence at all in the cost of the mixtures with negative carbon footprint.

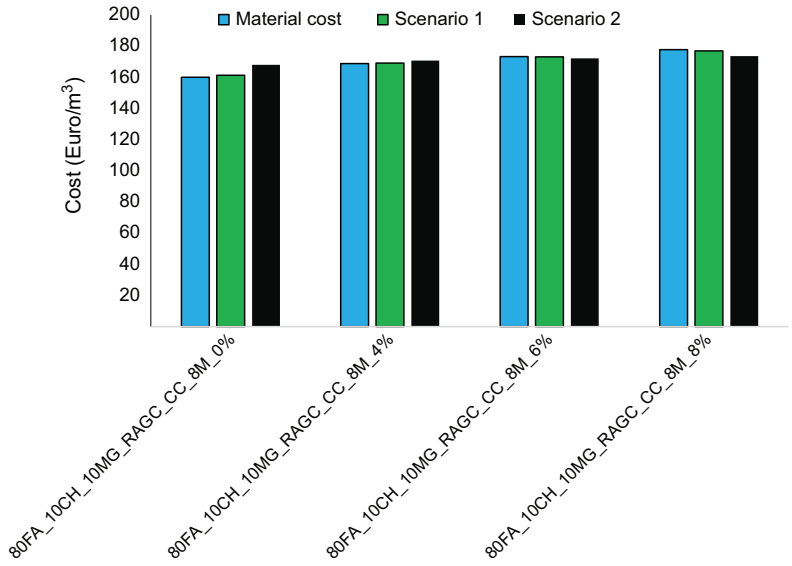

Figure 7.10 Cost of the mixtures.

Acknowledgments

The authors would like to acknowledge the financial support of the Foundation for Science and Technology (FCT) in the frame of project IF/00706/2014-UM.2.15.

References

Abdollahnejad, Z., Miraldo, S., Pacheco-Torgal, F., Barroso Aguiar, J., 2017. Cost-efficient one-part alkali-activated mortars with low global warming potential for floor heating systems applications". European Journal of Environmental and Civil Engineering 21, 412−429.

Agopyan, V., Savastano, H., John, V., Cincotto, M., 2005. Developments on vegetable fibre−cement based materials in São Paulo, Brazil: an overview. Cement and Concrete Composites 27, 527−536.

American Coal Ash Association, 2016. https://www.acaa-usa.org/Publications/Production-Use-Reports.

Arrigoni, A., Pelosato, R., Melià, P., Ruggieri, G., Sabbadini, S., Dotelli, G., 2017. Life cycle assessment of natural building materials: the role of carbonation, mixture components and transport in the environmental impacts of hempcrete blocks. Journal of Cleaner Production 149, 1051−1061.

ASTM C109/C109M-16a, 2016. Standard Test Method for Compressive Strength of Hydraulic Cement Mortars (Using 2-in. or [50-mm] Cube Specimens). ASTM International, West Conshohocken, PA. www.astm.org.

ASTM C618-15, 2015. Standard Specification for Coal Fly Ash and Raw or Calcined Natural Pozzolan for Use in Concrete. ASTM International, West Conshohocken, PA. www.astm.org.

Balčiūnas, G., Pundienė, I., Lekūnaitė-Lukošiūnė, L., Vėjelis, S., Korjakins, A., 2015. Impact of hemp shives aggregate mineralization on physical−mechanical properties and structure of composite with cementitious binding material. Industrial Crops and Products 77, 724−734.

Bendell, J., 2018. Deep adaptation: a map for navigating climate tragedy. In: Institute for Leadership and Sustainability (IFLAS) Occasional Papers, vol. 2. University of Cumbria, Ambleside, UK. http://insight.cumbria.ac.uk/id/eprint/4166/1/Bendell_DeepAdaptation.pdf.

Bernal, S., 2014. Resistance to carbonation of alkali-activated materials. In: Pacheco-Torgal, F., Labrincha, J.A., Leonelli, C., Palomo, A., Chindaprasirt, P. (Eds.), Handbook of Alkali-Activated Cements, Mortars and Concretes. WoodHead Publishing Limited- Elsevier Science and Technology, Abington Hall, Cambridge, UK, pp. 319−332.

Bernal, S., Rodríguez, E., Kirchheim, A., Provis, J., 2016. Management and valorisation of wastes through use in producing alkali-activated cement materials. Journal of Chemical Technology and Biotechnology. https://doi.org/10.1002/jctb.4927.

Bertos, M.F., Simons, S.J.R., Hills, C.D., Carey, P.J., 2004. A review of accelerated carbonation technology in the treatment of cement-based materials and sequestration of CO_2. Journal of Hazardous Materials 112 (3), 193−205.

Diquélou, Y., Gourlay, E., Arnaud, L., Kurek, B., 2015. Impact of hemp shiv on cement setting and hardening: influence of the extracted components from the aggregates and study of the interfaces with the inorganic matrix. Cement and Concrete Composites 55, 112−121.

El-Hassan, H., Shao, Y., 2015. Early carbonation curing of concrete masonry units with Portland limestone cement. Cement and Concrete Composites 62, 168−177.

Europe, 2019. 100 Radical Innovation Breakthroughs for the Future. https://ec.europa.eu/info/sites/info/files/research_and_innovation/knowledge_publications_tools_and_data/documents/ec_rtd_radical-innovation-breakthrough_052019.pdf.

Garcia-Lodeiro, I., Donatello, S., Fernandez-Jimenez, A., Palomo, A., 2016. Hydration of hybrid alkaline cement containing a very large proportion of fly ash: a descriptive model. Materials 9, 605.

Gram, H., 1983. Durability of Natural Fibres in Concrete. Stockolm: Swedish Cement and Concrete Research Institute.

Hansen, J., Sato, M., Kharecha, P., von Schuckmann, K., Beerling, D.J., Cao, J., Marcott, S., Masson-Delmotte, V., Prather, M.J., Rohling, E.J., Shakun, J., Smith, P., 2017. Young people's burden: requirement of negative CO_2 emissions. Earth System Dynamics Discussion arXiv preprint arXiv:1609.05878.

Ivanov, V., Alexeev, V., Koldunov, N.V., Repina, I., Sandø, A.B., Smedsrud, L.H., Smirnov, A., 2016. Arctic Ocean heat impact on regional ice decay: a suggested positive feedback. Journal of Physical Oceanography 46 (5), 1437−1456.

Jang, J.G., Kim, G.M., Kim, H.J., Lee, H.K., 2016. Review on recent advances in CO_2 utilization and sequestration technologies in cement-based materials. Construction and Building Materials 127, 762−773.

Li, Z., Wang, X., Wang, L., 2006. Properties of hemp fibre reinforced concrete composites. Composites part A: applied science and manufacturing 37 (3), 497−505.

Moore, F., Diaz, D., 2015. Temperature impacts on economic growth warrant stringent mitigation policy. Nature Climate Change 5, 127−131.

Mote, C., Dowling, J., Zhou, J., 2016. The power of an idea: the international impacts of the grand challenges for engineering. Engineering 2, 4−7.

Onuaguluchi, O., Banthia, N., 2016. Plant-based natural fibre reinforced cement composites: a review. Cement and Concrete Composites 68, 96−108.

Ouellet-Plamondon, C., Habert, G., 2014. Life cycle analysis (LCA) of alkali-activated cements and concretes. In: Pacheco-Torgal, F., Labrincha, J., Palomo, A., Leonelli, C., Chindaprasirt, P. (Eds.), Handbook of Alkali-Activated Cements, Mortars and Concretes. WoodHead Publishing-Elsevier, Cambridge, pp. 663−686.

Pacheco-Torgal, F., Jalali, S., 2011. Cementitious building materials reinforced with vegetable fibres: a review. Construction and Building Materials 25 (2), 575−581.

Pacheco-Torgal, F., Tam, V., Labrincha, J., Ding, Y., de Brito, J. (Eds.), 2013. Handbook of Recycled Concrete and Demolition Waste. Elsevier, Cambridge.

Payá, J., Monzó, J., Borrachero, M.V., Tashima, M.M., 2014. Reuse of aluminosilicate industrial waste materials in the production of alkali-activated concrete binders. In: Pacheco-Torgal, F., Labrincha, J., Palomo, A., Leonelli, C., Chindaprasirt, P. (Eds.), Handbook of Alkali-Activated Cements, Mortars and Concretes. WoddHead Publishing, Cambridge, UK, pp. 487−518.

Provis, J.L., 2014. Geopolymers and other alkali activated materials: why, how, and what ? Materials and Structures 47, 11−25.

Šavija, B., Luković, M., 2016. Carbonation of cement paste: understanding, challenges, and opportunities. Construction and Building Materials 117, 285−301.

Screen, J.A., Deser, C., 2019. Pacific Ocean variability influences the time of emergence of a seasonally ice-free Arctic ocean. Geophysical Research Letters 46 (4), 2222−2231.

Sedan, D., Pagnoux, C., Smith, A., Chotard, T., 2008. Mechanical properties of hemp fibre reinforced cement: influence of the fibre/matrix interaction. Journal of the European Ceramic Society 28, 183−192.

Shea, A., Lawrence, M., Walker, P., 2012. Hygrothermal performance of an experimental hemp-lime building. Construction and Building Materials 36, 270−275.

Stanford Report, 2015. Estimated Social Cost of Climate Change Not Accurate, Stanford Scientists Say. Retrieved from: http://news.stanford.edu/news/2015/january/emissions-social-costs-011215.html. (Accessed 14 June 2017).

Tabone, I., Robinson, A., Alvarez-Solas, J., Montoya, M., 2019. Submarine melt as a potential trigger of the North East Greenland ice stream margin retreat during marine isotope stage 3. The Cryosphere 13 (7), 1911−1923.

Tonoli, G., Santos, S., Joaquim, A., Savastano, H., 2010. Effect of accelerated carbonation on cementitious roofing tiles reinforced with lignocellulosic fibre. Construction and Building Materials 24, 93−201.

Turetsky, M.R., Abbott, B.W., Jones, M.C., Anthony, K.W., Olefeldt, D., Schuur, E.A., Koven, C., McGuire, A.D., Grosse, G., Kuhry, P., Hugelius, G., 2019. Permafrost Collapse is Accelerating Carbon Release.

Valle-Zermeño, R., Aubert, J.E., Laborel-Préneron, A., Formosa, J., Chimenos, J.M., 2016. Preliminary study of the mechanical and hygrothermal properties of hemp-magnesium phosphate cements. Construction and Building Materials 105, 62−68.

Wadhams, P., 2017. A Farewell to Ice. Oxford University Press, Oxford.

Watts, J., 2018. Arctic Warming: Scientists Alarmed by 'crazy' Temperature Rises, vol. 27. The Guardian.

Xu, Y., Ramanathan, V., Victor, D.G., 2018. Global Warming Will Happen Faster than We Think.

Zhang, Z., Huisingh, D., 2017. Carbon dioxide storage schemes: technology, assessment and development. Journal of Cleaner Production 142, 1055−1064.